


Structural Connectivity Differences in Motor Network Between Tremor-Dominant and Nontremor Parkinson's Disease

Gaetano Barbagallo,^{1†} Maria Eugenia Caligiuri,^{2†} Gennarina Arabia,¹
Andrea Cherubini,² Angela Lupo,¹ Rita Nisticò,² Maria Salsone,²
Fabiana Novellino,² Maurizio Morelli,¹ Giuseppe Lucio Cascini,³
Domenico Galea,³ and Aldo Quattrone ^{1,2*}

¹Institute of Neurology, University "Magna Graecia", Catanzaro, Italy

²Neuroimaging Research Unit, Institute of Molecular Bioimaging and Physiology,
National Research Council, Catanzaro, Italy

³Institute of Radiology, Nuclear Medicine Unit, University "Magna Graecia",
Catanzaro, Italy

Abstract: Motor phenotypes of Parkinson's disease (PD) are recognized to have different prognosis and therapeutic response, but the neural basis for this clinical heterogeneity remains largely unknown. The main aim of this study was to compare differences in structural connectivity metrics of the main motor network between tremor-dominant and nontremor PD phenotypes (TD-PD and NT-PD, respectively) using probabilistic tractography-based network analysis. A total of 63 PD patients (35 TD-PD patients and 28 NT-PD patients) and 30 healthy controls underwent a 3 T MRI. Next, probabilistic tractography-based network analysis was performed to assess structural connectivity in cerebello-thalamo-basal ganglia-cortical circuits, by measuring the connectivity indices of each tract and the efficiency of each node. Furthermore, dopamine transporter single-photon emission computed tomography (DAT-SPECT) with ¹²³I-ioflupane was used to assess dopaminergic striatal depletion in all PD patients. Both PD phenotypes showed nodal abnormalities in the substantia nigra, in agreement with DAT-SPECT evaluation. In addition, NT-PD patients displayed connectivity alterations in nigro-pallidal and fronto-striatal pathways, compared with both controls and TD-PD patients, in which the same motor connections seemed to be relatively spared. Of note, in NT-PD group, rigidity-bradykinesia score correlated with fronto-striatal connectivity abnormalities. These findings demonstrate that structural connectivity alterations occur in the cortico-basal ganglia circuit of NT-PD patients, but not in TD-PD patients, suggesting that these anatomical differences may underlie different motor phenotypes of PD. *Hum Brain Mapp* 38:4716–4729, 2017. © 2017 Wiley Periodicals, Inc.

Key words: Parkinson's disease; motor phenotypes of Parkinson's disease; probabilistic tractography; structural network analysis; dopamine transporter single-photon emission computed tomography; tremor-dominant Parkinson's disease; nontremor Parkinson's disease

*Correspondence to: Prof. Aldo Quattrone, Institute of Neurology, University Magna Graecia of Catanzaro, Viale Europa, 88100 Catanzaro, Italy. E-mail: quattrone@unicz.it

†These authors contributed equally to this work.

Received for publication 6 April 2017; Revised 25 May 2017; Accepted 13 June 2017.

DOI: 10.1002/hbm.23697

Published online 20 June 2017 in Wiley Online Library (wileyonlinelibrary.com).

INTRODUCTION

The classical triad of motor symptoms of Parkinson's disease (PD) includes resting tremor, rigidity, and bradykinesia [Parkinson, 1817]. However, the expression of these cardinal motor symptoms varies markedly between patients [Hoehn and Yahr, 1967], and it is possible to distinguish two main clinical phenotypes, a tremor-dominant subtype (TD-PD) and a nontremor subtype (NT-PD), in which akinetic-rigid symptoms are predominant [Burn et al., 2006; Jankovic et al., 1990; Jellinger and Paulus, 1992; Lewis et al., 2005; Zetuský et al., 1985]. Moreover, clinical and epidemiological evidences suggest that the motor phenotype may be predictive of clinical course and prognosis [Foltynie et al., 2002; Nicoletti et al., 2010]. In fact, with respect to TD-PD, NT-PD has a more rapid rate of progression with an increased risk to develop disability and cognitive impairment [Aarsland et al., 2003; Burn et al., 2006; Goetz et al., 1988; Jankovic and Kapadia, 2001; Williams-Gray et al., 2007].

The neural basis for this clinical heterogeneity of PD remains unknown. Functional magnetic resonance imaging (fMRI) studies clearly demonstrated that the activation at the level of the prefrontal cortex and the globus pallidus was reduced in patients with NT-PD compared to those with TD-PD and controls [Prodoehl et al., 2013]. On the other hand, in TD-PD patients, cerebral activity related to tremor first arised in the internal globus pallidus and was then propagated to the cerebello-thalamo-cortical loop, the "dimmer-switch hypothesis" [Dirkx et al., 2016; Helmich et al., 2011, 2012].

However, it is not yet clear whether the functional changes within these motor circuits are concordant with anatomical connectivity modifications.

To date, only one recent study investigated the presence of reduced cortical-subcortical sensorimotor connectivity in PD patients compared to controls using probabilistic tractography [Sharman et al., 2013], but no direct comparison of structural brain network properties has been performed in motor phenotypes of PD. This work was designed to investigate structural differences in the main motor network between patients with NT-PD and patients with TD-PD. This motor system, including cerebello-thalamo-cortical and cortico-basal ganglia circuits [Lewis et al., 2011; Obeso et al., 2014], was explored by using probabilistic tractography-based structural network analysis. We hypothesized that patients with NT-PD would show structural abnormalities compared to patients with TD-PD and healthy controls. We also quantified dopaminergic striatal depletion in all patients using dopamine transporter single-photon emission computed tomography (DAT-SPECT) with ^{123}I -ioflupane. Furthermore, we tested the hypothesis that the structural and functional neuroimaging parameters (i.e., MRI network metrics and ^{123}I -ioflupane uptakes, respectively) would be differently associated with the motor signs in the two phenotypes of PD.

MATERIAL AND METHODS

Subjects

Three groups of 35 TD-PD patients, 28 NT-PD patients, and 30 controls were enrolled in the study.

Patients were included when they had idiopathic PD, diagnosed according to the UK Brain Bank criteria [Hughes et al., 1992]. Exclusion criteria were as follows: (1) cognitive impairment (Mini Mental State Examination [MMSE] [Folstein et al., 1975] score < 24); (2) neurological, cerebrovascular or thyroid comorbidities; (3) moderate to severe head tremor and/or dyskinesias; (4) normal functional neuroimaging of the presynaptic dopaminergic system; and (5) treatment with deep brain stimulation and general exclusion criteria for MRI scanning. Motor disability was assessed using Motor Examination scores of the Unified Parkinson's Disease Rating Scale (UPDRS-ME) [Fahn et al., 1987]. TD-PD was defined as a UPDRS-ME resting tremor score ≥ 2 for at least 1 upper or lower extremity during physical examination, and a history of resting tremor. NT-PD was defined by a UPDRS-ME resting tremor score of 0 during physical examination, and as no history of resting tremor [Helmich et al., 2011; Prodoehl et al., 2013]. A levodopa equivalent daily dose (LEDD) [Tomlinson et al., 2010] was calculated for each patient under anti-Parkinsonian therapy. We assessed patients' clinical disability in the "practically off" condition that was at least 12 h after the last dose [Langston et al., 1992].

Controls were defined as a no history of neurological or severe general medical diseases, an MMSE ≥ 24 and a UPDRS-ME = 0.

All participants gave written informed consent, which was approved by the Ethical Committee of the University "Magna Graecia" of Catanzaro, according to the Helsinki Declaration.

DAT-SPECT

PD patients underwent a DAT-SPECT scan within 2 weeks before or after the MRI scan. DAT-SPECT acquisition and processing procedures were performed according to the European Association of Nuclear Medicine guidelines. Patients received perchlorate (1,000 mg) 30 min before scanning to block thyroid uptake of free radioactive iodine. Brain imaging was performed 3 hours after the administration of 200 MBq of ^{123}I -ioflupane (GE-Amersham, Eindhoven, The Netherlands) using a dual-headed gamma camera (Infinia Hawkeye; General Electric, Milwaukee, WI) equipped with low-energy, high-resolution collimators. Scans were acquired with a photopeak window centered on 159 keV $\pm 10\%$ with a 128×128 image matrix (zoom factor: 1.5; 40 s per view and 2×64 views). Slice thickness was 2.95 mm. Patients were carefully positioned in the gamma camera, with their meato-orbital axis in a transverse plane to reduce reorientation during reconstruction, in a special head holder that allowed a minimal rotation distance. Images were

reconstructed using filtered back projection with a Butterworth filter (cutoff 0.5 and order 6). Chang's correction method was used to compensate for attenuation using a coefficient of 0.11 cm^{-1} . The average total number of counts was 1.8–2.0 million for each SPECT study. Regions of interest (ROIs) were depicted on reoriented, attenuation-corrected images by using the DATSCAN 3 tool (v.2 for Xeleris workstation; General Electric). First, the three consecutive slices where striatum was best represented were selected. Afterward, four striatal ROIs were manually superimposed on the corresponding brain regions in the central slice. These preset ROIs have fixed shape and dimensions (twice the full-width at half-maximum [FWHM]), as previously suggested [Darcourt et al., 2010], but they may be rotated on the axial plane to obtain the best fit to the target region. ROIs were visually centered on the pixels with higher uptake. Finally, the occipital ROI is positioned and the five regions are copied on two consecutive slices. Specific-to-nonspecific binding was evaluated through ratios between specific uptake in striatal ROIs and mean occipital ROI uptake. ROI values were considered both individually for the right and left hemisphere. A semiquantitative assessment was performed. ROIs with fixed sizes were superimposed on the striatum (left and right caudate nucleus, left and right putamen) and on occipital cortex, that has a low number of DAT binding sites, and it is a useful reference region. The asymmetry of striatal dopamine depletion was evaluated, both visually and through the binding ratios, to identify the more affected and the less affected side for each patient (MAS and LAS, respectively).

MRI

Acquisition

All participants underwent the same MRI scanning protocol using a 3-T GE-MR750 scanner (GE Healthcare, Rahway, NJ). PD patients underwent MRI in the “practically off” condition. Head movements were minimized using foam pads around participants' heads. The protocol included a whole-brain T1-weighted scan [SPGR; TE/TR = 3.7/9.2 ms, flip angle 128, voxel-size $1.0 \times 1.0 \times 1.0 \text{ mm}^3$]; a diffusion-weighted scan that was acquired using a spin-echo echo-planar imaging sequence (TE/TR 81/10050 ms, band-width 250 kHz, matrix size 128×128 ; 80 axial slices, voxel size $2.0 \times 2.0 \times 2.0 \text{ mm}^3$) with 27 isotropically distributed orientations for the diffusion-sensitizing gradients at a b -value of 1000 s/mm^2 ; conventional T2-weighted and FLAIR sequences. All images were inspected by an expert to exclude excessive motion artifacts or presence of brain abnormalities. FLAIR, T2-weighted, and T1-weighted images were visually checked to assess vascular lesions for each patient. The extent and possible etiology of white matter hyperintensities were not different across patients, independent of the group.

Motor network reconstruction

Image processing was performed using the Functional Magnetic Resonance Imaging of the Brain (FMRIB) Analysis Group Software Library (FSL) (Oxford University, United Kingdom) [Jenkinson et al., 2012]. The MRI processing workflow is shown in Figure 1. Structural T1 images were skull-stripped and then used to identify the different regions composing the motor circuit. In particular, for each subject, the following subcortical structures were segmented using the FIRST tool of FSL [Patenaude et al., 2011]: left and right caudate, left and right putamen, and left and right globus pallidus. Thalamic ROI included two ventrolateral subthalamic regions that were selected from the *Thalamic Connectivity Atlas* of FSL, according to their connectivity with premotor and primary motor cortices. The Substantia nigra was identified by means of a probabilistic atlas derived from MRI data of fifty healthy volunteers [Murty et al., 2014]. Cortical and cerebellar motor regions, instead, were identified using the AAL116 atlas; in particular, we extracted the precentral gyrus, which includes the premotor and primary motor cortices, the supplementary motor area, and a further ROI including the motor lobules of the cerebellum (IV, V, VI, VIII), as in Buijink et al. [2015].

Atlas-based ROIs were warped in each subject's T1 space as follows: first, the atlas was nonlinearly registered to each subject's T1 image by using the FNIRT tool of FSL [Jenkinson et al., 2012]; afterward, the resulting warp field was applied to the binary masks localizing the ROIs. The resulting images were visually assessed on T1- and T2-weighted (co-registered to T1) images by one trained expert to exclude misregistration or erroneous ROIs identification. In subsequent analyses, left and right motor circuits were analyzed separately, mainly to avoid spurious reconstructions of invalid connections. Each motor cerebellar hemisphere was included in the contralateral circuit, since studies on both primates and humans have demonstrated that the thalamo-cerebellar connections decussate at the level of the red nucleus [Bostan et al., 2010; Buijink et al., 2015; Pelzer et al., 2013].

Diffusion-weighted data were corrected for distortion and movement artefacts, and subsequently used to perform probabilistic tractography of the motor network. Head motion and image distortions induced by eddy currents in the DTI data were corrected by applying a 3D full-affine (mutual-information cost function) alignment of each image to the mean no-diffusion-weighting (b_0) image. After distortions correction, DTI data were averaged and concatenated into 28 (1 mean b_0 + 27 b_{1000}) volumes. To reconstruct connections in the motor circuit with probabilistic tractography, Bayesian Estimation of Diffusion Parameters Obtained using Sampling Techniques (bedpostX tool of FSL) [Behrens et al., 2003, 2007] was performed on diffusion data, which allows the modeling of crossing fibres within each voxel of the brain. Briefly, Markov Chain Monte-Carlo sampling was used to build up distributions on diffusion parameters at

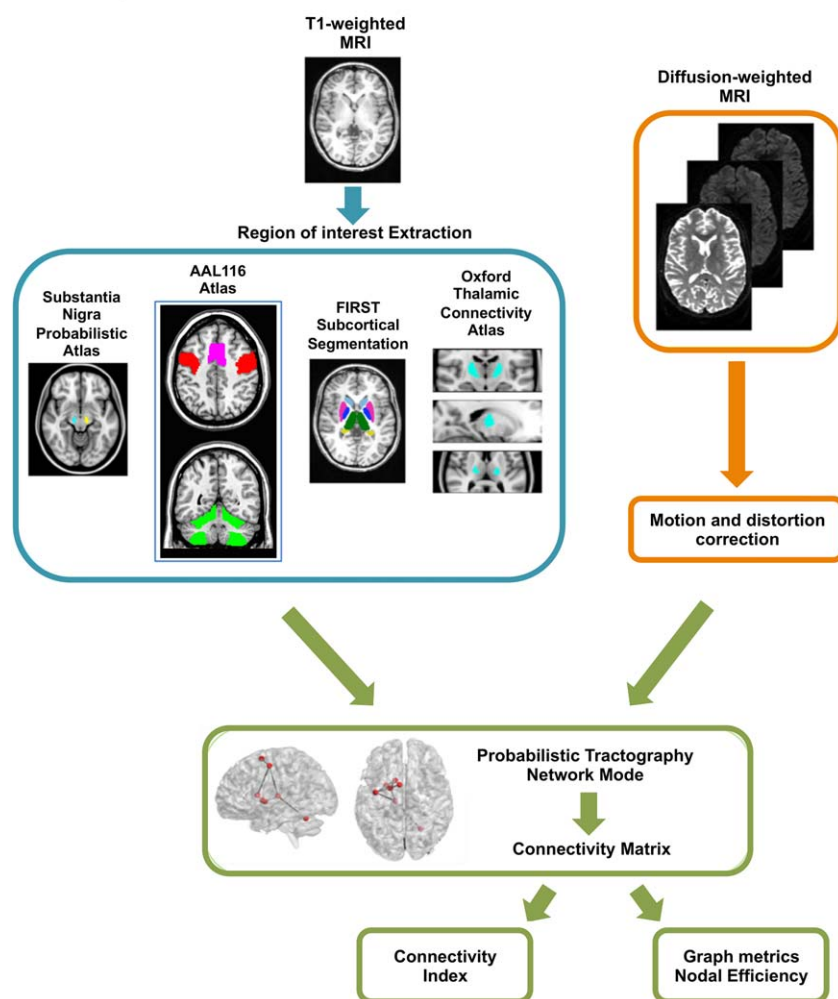


Figure 1.

MRI processing workflow. AAL, automated anatomical labeling; MRI, magnetic resonance imaging; FIRST, Bayesian segmentation of subcortical structures. [Color figure can be viewed at wileyonlinelibrary.com]

each voxel. This processing step, necessary for probabilistic tractography, was carried out with default options [Behrens et al., 2007], that is, two fibres modeled per voxel and 1000 iterations before starting the sampling (burning period). Once bedpostX was completed, the probtrackX tool was used to generate connectivity distributions between all the ROIs in the motor circuit. This was done by running probabilistic tractography in network-mode and by setting all the ROIs of the circuit as waypoint and termination masks, thus ensuring that probabilistic pathways generating from each seed ROI were accepted only if they reached, and terminated in, at least one of the other regions of the network. Furthermore, as we focused on the left and right circuit separately, we also set an exclusion criterion for streamlines reaching the forebrain region of the midsagittal plane: this allowed excluding streamlines that from one hemisphere

reached for the contralateral one, except in the case of streamlines from the contralateral motor cerebellum. Probabilistic tractography was performed with the following default parameters, based on the algorithm's (probtrackx) default usage: 5000 streamlines drawn, from each voxel, through the probability distributions on principal fibres direction, output of bedpostX; 0.2 curvature threshold, which represents the cosine of the minimum allowed angle between two steps; exclusion of pathways that create loops, traveling over voxels where they have already been; samples are terminated after 2000 steps, where each step has a length of 0.5 mm.

Probabilistic tractography in network mode provided, for each subject, a connectivity matrix with dimensions equal to the number of ROIs in each circuit (eight in this case). Each entry ij of the matrix represented the number

of streamlines connecting the i -th and j -th ROI. These values were normalized, to take into account differences in the seed-ROI sizes, by dividing each row of the matrix for the waytotal of the corresponding ROI, that is, the total number of streamlines drawn from it and surviving all the constraints of tractography (waypoints, termination mask, and exclusion mask). Thus, we obtained for each reconstructed tract an anatomical connectivity index, which is an indirect measure of tract integrity.

The computation of normalized connectivity matrices allowed us to explore the network properties of the motor circuit. However, applying graph analysis to tractography data requires the choice of a specific connection density, to take into account the influence of intersubject variability in the total number of reconstructed streamlines. If the appropriate density were not used, each subject's raw connectivity matrix would show substantial differences based on slight variations in individual anatomy. In this work, we imposed a "subject" threshold and a "matrix" threshold. The "subject" threshold was chosen to retain only connections present in at least 50% of the study participants, thus avoiding influences due to individual anatomy. The "matrix" threshold, instead, was chosen over a range of probability values, that is, from 0.001 (more loose) to 0.01 (more stringent). As our study focuses on a very specific network, we chose the most stringent threshold of 0.01 with the aim of decreasing the risk of erroneous findings due to the presence of spurious connections [Wen et al., 2011].

Normalized networks allow for topological properties, such as path length, to be quantitatively compared across subjects. We calculated graph metrics using the brainGraph toolbox available in R (<https://github.com/cwatson/brainGraph>). The definition of these measures has been discussed in detail elsewhere [Bullmore and Sporns, 2009]. We analysed the structural motor network by measuring the weighted efficiency of each node. The nodal efficiency is inversely proportional to the path length of connections between a given node and every other node in the network, and can be interpreted as inversely related to the dispersion of the signal along the paths that connect each node. The nodal efficiency was weighted by the connectivity indices of the tracts starting from the node [Achard and Bullmore, 2007].

Statistical Analysis

Statistical analyses were performed with Statistical Package for Social Science Software (SPSS, version 12.0, Chicago, IL, USA) for Windows.

Comparative analyses

Clinical variables. To compare sex distributions among groups, we used the χ^2 test, whereas for age and MMSE score, one-way ANOVA and the Kruskal–Wallis test were performed, respectively. The differences in disease duration, LEDD, H&Y, UPDRS-ME, and UPDRS-ME subscores

between PD subgroups were assessed by using the Mann–Whitney U test, whereas for age at onset, the unpaired t test was used.

^{123}I -ioflupane uptake values. To investigate the differences in LAS and MAS striata ^{123}I -ioflupane uptake values between PD subgroups, we used the unpaired t test and the Mann–Whitney U test for normally and non-normally distributed variables, respectively.

MRI network metrics. For each patient with PD, we elected an MAS and an LAS that were ipsilateral to the more affected and less affected striata at DAT-SPECT. To compare the differences in anatomical connectivity indices and weighted nodal efficiency values among groups, we used analysis of covariance, with age, sex, and total intracranial volume included as covariates. We considered the MAS and LAS for patients with Parkinson's disease and the average of right and left side for control subjects. Significance level was set at 0.05 after false discovery rate (FDR) correction for multiple comparisons [Benjamini and Hochberg, 1995].

Correlation analyses

To explore the relationships of clinical variables with structural and functional neuroimaging parameters in patients with PD, we calculated the Spearman rank correlation coefficient. Over the PD subgroups, we considered UPDRS-ME subscores of more severely affected limbs. The correlations were considered statistically significant if the relative P values were <0.05 after FDR correction [Benjamini and Hochberg, 1995].

RESULTS

Intergroup Comparisons

Clinical data

Subject characteristics are shown in Table I. No significant differences were found between groups in demographics or clinical data, except for the UPDRS-ME subscores. As expected, patients with NT-PD displayed significantly lower values of tremor subscore and higher values of nontremor subscore (B + R) compared with those with TD-PD, whereas the amount of dopaminergic medication, UPDRS-ME, and Hohen and Yahr (H&Y) scores were similar between the two phenotypes. In all PD patients, the more severely affected limbs were always contralateral to the side most affected by striatal depletion as seen on DAT-SPECT.

DAT-SPECT data

Patients with NT-PD showed significantly lower ^{123}I -ioflupane uptakes values in the LAS caudate nucleus compared to those with TD-PD (Table I). No other significant difference was found between the two phenotypes.

TABLE I. Clinical and DAT-SPECT features of the study subjects^a

	Controls (<i>n</i> = 30)	All PD (<i>n</i> = 63)	PD phenotypes		<i>P</i> value
			TD-PD (<i>n</i> = 35)	NT-PD (<i>n</i> = 28)	
Sex, M/F	20/10	42/21	26/9	16/12	ns ^b
Age, y	66.3 ± 6.7	66.2 ± 8.3	66.2 ± 8.4	66.3 ± 8.2	ns ^c
MMSE	27.0 ± 6.3	27.0 ± 2.0	26.8 ± 2.0	27.3 ± 1.9	ns ^d
Age at onset, y		62.1 ± 7.9	62.4 ± 7.8	61.6 ± 8.3	ns ^e
Disease duration, y		4.2 ± 3.3	3.8 ± 2.9	4.6 ± 3.8	ns ^f
LEDD, mg/die		245.6 ± 292.9	178.0 ± 226.2	330.2 ± 345.4	ns ^f
H&Y		1.9 ± 0.5	1.8 ± 0.5	2.0 ± 0.6	ns ^f
UPDRS-ME		23.4 ± 10.0	23.5 ± 9.8	23.2 ± 10.5	ns ^f
Tremor subscore		4.1 ± 3.9	6.7 ± 3.3	0.7 ± 1.0	<0.001 ^f
Non-tremor subscore (B+R)		13.4 ± 7.3	11.1 ± 5.6	16.4 ± 8.3	0.004 ^f
Axial subscore		5.8 ± 3.2	5.6 ± 2.7	6.1 ± 3.8	ns ^f
DAT-SPECT features					
LAS putamen		2.5 ± 0.7	2.7 ± 0.6	2.4 ± 0.7	ns ^f
MAS putamen		2.1 ± 0.4	2.1 ± 0.4	2.0 ± 0.4	ns ^e
LAS caudate nucleus		3.4 ± 0.9	3.7 ± 0.8	3.1 ± 1.0	0.008 ^e
MAS caudate nucleus		3.1 ± 0.8	3.3 ± 0.7	3.0 ± 0.8	ns ^e
LAS striatum		3.0 ± 0.7	3.1 ± 0.7	2.9 ± 0.8	ns ^e
MAS striatum		2.6 ± 0.5	2.7 ± 0.5	2.5 ± 0.5	ns ^e

Abbreviations: DAT-SPECT = dopamine transporter single-photon emission computed tomography; PD = Parkinson's disease; TD-PD = patients with tremor-dominant Parkinson's disease; NT-PD = patients with nontremor Parkinson's disease; M = male; F = female; MMSE = Mini Mental State Examination; LEDD = levodopa equivalent daily dose; H&Y = Hohen and Yahr scale; UPDRS-ME = Unified Parkinson's Disease Rating Scale-Motor Examination; Tremor subscore = resting and postural tremor (sum of UPDRS items 20–21); Nontremor subscore (B + R) = limb bradykinesia and rigidity (sum of UPDRS items 22–26); axial subscore = axial symptoms (sum of UPDRS items 18, 19, 22, 27–31); LAS = less affected side; MAS = more affected side; *ns* = not significant.

Nine NT-PD patients had a very subtle postural tremor while off-medication at the day of testing, explaining the nonzero tremor subscore. The DAT-SPECT values were determined using the ratio of specific to nonspecific (occipital area) radioligand binding.

^aata are given as mean values ± standard deviation.

^bχ² test.

^cOne way ANOVA.

^dKruskal-Wallis test.

^eUnpaired *t* test.

^fMann-Whitney *U* test.

MRI connectivity data

Figure 2 and Table II show the main results of the comparative analysis of MRI network metrics in the more affected hemisphere.

For what concerns the connectivity indices, the values of the globus pallidus–substantia nigra, putamen–precentral cortex, and caudate nucleus–supplementary motor area tracts were significantly lower in patients with NT-PD compared to both TD-PD patients and controls; the values of the globus pallidus–thalamus tract were significantly lower in patients with NT-PD compared to controls, and the values of the thalamus–precentral cortex tract were significantly lower in patients with NT-PD compared to those with TD-PD. It is notable that the caudate nucleus–supplementary motor area tract could not be reconstructed in any patient with NT-PD.

For what concerns the weighted nodal efficiency, the values of the globus pallidus were significantly higher in patients with NT-PD compared to both TD-PD patients

and controls; the values of the supplementary motor area and the putamen were significantly higher in patients with NT-PD compared to controls; the values of the substantia nigra were significantly higher in both PD phenotypes compared to controls.

No significant differences were observed among the groups regarding any of the MRI network metrics of the less-affected hemisphere, except that NT-PD patients had significantly higher weighted nodal efficiency values in the substantia nigra compared to control subjects (Table II).

Intragroup Correlations

Figure 3 shows the main results of the correlation analysis in the entire PD cohort and in the PD subgroups (for more details, see also Tables III and IV).

Over the entire PD cohort, striatal ¹²³I-ioflupane uptakes correlated with disease duration, UPDRS-ME, and nontremor subscore (B + R), but not with tremor subscore. Correlations

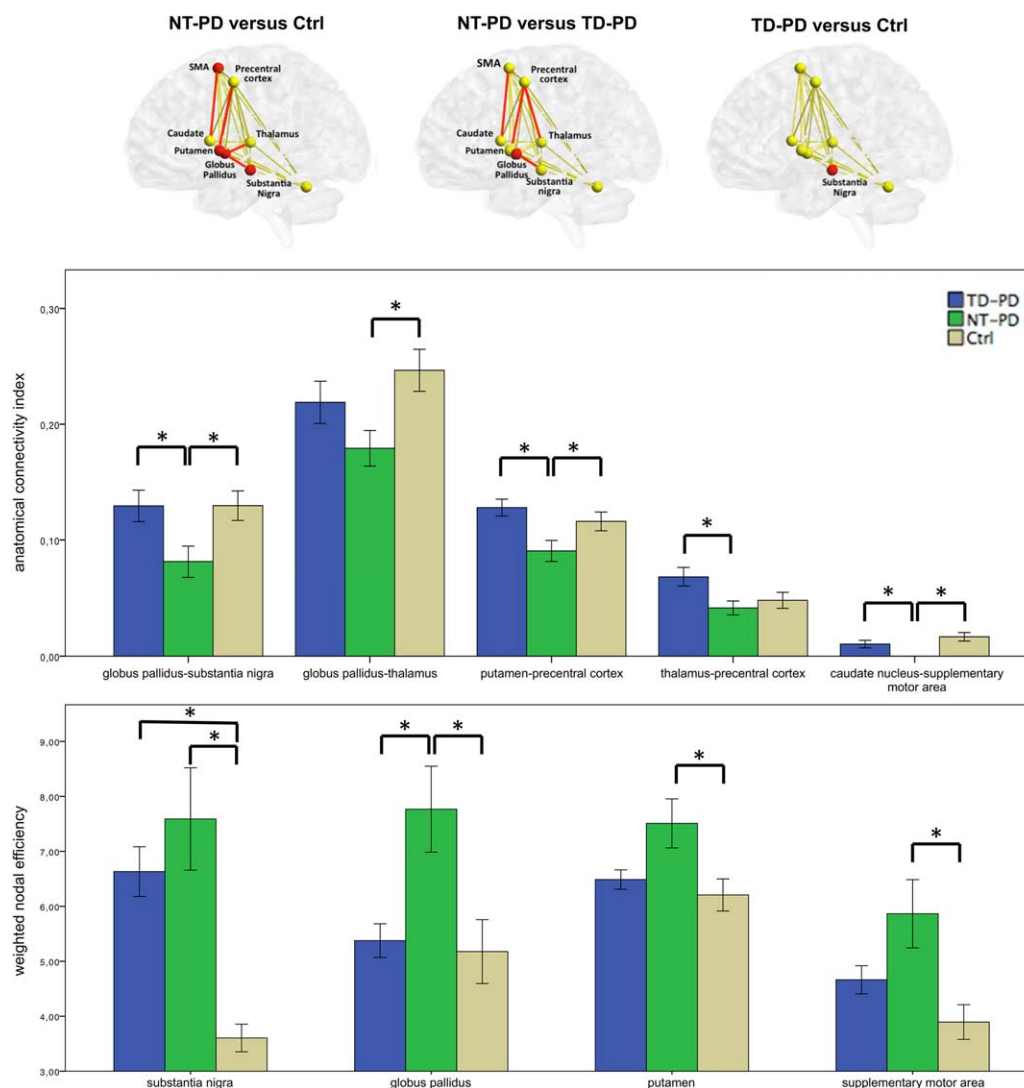


Figure 2.

Group differences in MRI network metrics (i.e., connectivity index and weighted nodal efficiency). Spheres and lines represent brain nodes and edges, with red spheres and red lines indicating respectively the nodes and the edges showing significance between groups (top). Anatomical connectivity index and weighted nodal efficiency mean values for each brain edges and nodes, respectively (bottom). Regarding the MRI network metrics in the figure, we

considered the more affected side for patients with Parkinson's disease, and the average of right and left side for control subjects. NT-PD, patients with nontremor Parkinson's disease; TD-PD, patients with tremor-dominant Parkinson's disease; *P value <0.05 after false discovery rate correction. [Color figure can be viewed at wileyonlinelibrary.com]

between striatal ¹²³I-ioflupane uptakes and nontremor subscore (B + R) persisted also in the PD subgroups.

Over the PD subgroups, the correlation analysis between the UPDRS-ME subscores of more severely affected limbs and MRI network metrics showed that, in patients with NT-PD, the bradykinesia-rigidity severity correlated negatively with the connectivity indices of putamen-precentral cortex tract, and positively with putaminal weighted nodal efficiency values; whereas, in patients with TD-PD,

the tremor severity correlated positively with the connectivity indices of globus pallidus-substantia nigra tract, and negatively with the pallidal weighted nodal efficiency values.

DISCUSSION

This study examined structural differences in the main brain motor network between patients with TD-PD and

TABLE II. Altered MRI network metrics (i.e., weighted nodal efficiency values and anatomical connectivity indices) of patients with Parkinson's disease

MRI network metrics Anatomical connectivity indices (mean ± SE)	Ctrls ^a (n = 30)	TD-PD (n = 35)	NT-PD (n = 28)	P value		
				NT-PD vs Ctrl	NT-PD vs TD-PD	TD-PD vs Ctrl
MAS globus pallidus–substantia nigra tract	0.13 ± 0.01	0.13 ± 0.01	0.08 ± 0.01	0.03	0.03	ns
MAS globus pallidus–thalamus tract	0.25 ± 0.02	0.22 ± 0.02	0.18 ± 0.02	0.02	ns	ns
MAS putamen–precentral cortex tract	0.12 ± 0.01	0.13 ± 0.01	0.09 ± 0.01	0.05	0.02	ns
MAS thalamus–precentral cortex tract	0.05 ± 0.01	0.07 ± 0.01	0.04 ± 0.01	ns	0.02	ns
MAS caudate nucleus–supplementary motor area tract	0.01 ± 0.003	0.01 ± 0.003	0.00 ± 0.00	0.01	0.02	ns
Weighted nodal efficiency values (mean ± SE)						
MAS globus pallidus	5.18 ± 0.58	5.38 ± 0.31	7.77 ± 0.78	0.01	0.02	ns
MAS putamen	6.21 ± 0.29	6.49 ± 0.18	7.51 ± 0.45	0.03	ns	ns
MAS supplementary motor area	3.89 ± 0.32	4.66 ± 0.27	5.86 ± 0.62	0.02	ns	ns
MAS substantia nigra	3.60 ± 0.25	6.63 ± 0.45	7.59 ± 0.93	0.01	ns	0.02
LAS substantia nigra	3.60 ± 0.25	4.85 ± 0.29	4.94 ± 0.55	0.02	ns	ns

Abbreviations: Ctrls = control subjects; TD-PD = patients with tremor-dominant Parkinson's disease; NT-PD = patients with nontremor Parkinson's disease; MAS = more affected side; LAS = less affected side; ns = not significant.

Significant *P* values corrected for multiple comparisons (false discovery rate correction) are indicated in bold.

^aThe average of right and left hemispheres was considered for control group.

those with NT-PD, using probabilistic tractography. There are two main findings. First, NT-PD patients showed structural connectivity alterations in the cortico-basal ganglia circuits with nigro-pallidal and fronto-striatal involvement, whereas the same motor connections seemed to be relatively spared in the TD-PD group. Second, the severity of rigidity-bradykinesia was inversely related to connectivity indices of fronto-striatal tract, indicating a major role of the cortico-basal ganglia motor circuits in the pathophysiology of this symptom. In addition, in NT-PD patients, weighted nodal efficiency, that is inversely proportional to the number of connections starting from each node, was markedly altered at the level of globus pallidus, putamen, and supplementary motor area. Similarly to the structural connectivity changes, weighted nodal efficiency was normal in TD-PD patients, whose values did not significantly differ from controls.

The reduced connectivity indices of the nigro-pallidal tract and the increased pallidal weighted nodal efficiency values found in NT-PD patients could be due to damage of the nigral dopaminergic neurons projecting to the globus pallidus (nigro-pallidal pathway) [Lindvall and Björklund, 1979; Parent et al., 1990]. The alteration of pallidal connectivity in NT-PD patients, along with its relative integrity in TD-PD, is not surprising and it is consistent with previous pathological findings of reduced dopamine levels in the ventral part of the internal globus pallidus in NT-PD patients compared with TD-PD patients [Rajput et al., 2008]. Our finding is also in agreement with previous functional MRI findings [Prodoehl et al., 2013], in which early-stage, drug-naive NT-PD patients had reduced activity in the internal and the external globus pallidus with respect to early-stage, drug-naive TD-PD patients and

controls. Interestingly, we also found a significant decrease in the connectivity index of the pallido-thalamic tract in NT-PD patients, which could represent an indirect damage secondary to the nigro-pallidal dysfunction.

In addition to the globus pallidus, patients with NT-PD showed also structural connectivity changes in the fronto-striatal pathways and increased weighted nodal efficiency values of putamen and supplementary motor area, while these connectivity alterations were spared in TD-PD, who showed metrics values similar to those detected in controls. More in detail, our tractography analysis also showed a decrease in connectivity indices of the putamen-precentral cortex tract, and of the caudate nucleus-supplementary motor area tract in NT-PD patients. This result indicates that the impairment of the cortico-striatal projections might be more severe in akinetic-rigid phenotype. Striatum (i.e., putamen and caudate nucleus) receives projections from frontal motor areas (i.e., primary motor cortex, premotor cortex, and supplementary motor area), which are involved in preparation and execution of the movements [DeLong and Wichmann, 2015; Haber, 2016]. Furthermore, the significant correlation of rigidity-bradykinesia subscores of more severely affected limbs with putaminal weighted nodal efficiency values and putamen-precentral cortex tract connectivity indices in NT-PD patients further strengthens the importance of fronto-striatal involvement in the emergence of bradykinesia and rigidity, which may result from a failure of basal ganglia output to reinforce the cortical mechanisms that prepare and execute the commands to move [Berardelli et al., 2001; Michely et al., 2015].

The involvement of the substantia nigra as a node was similar in both subgroups and for both sides, compared to

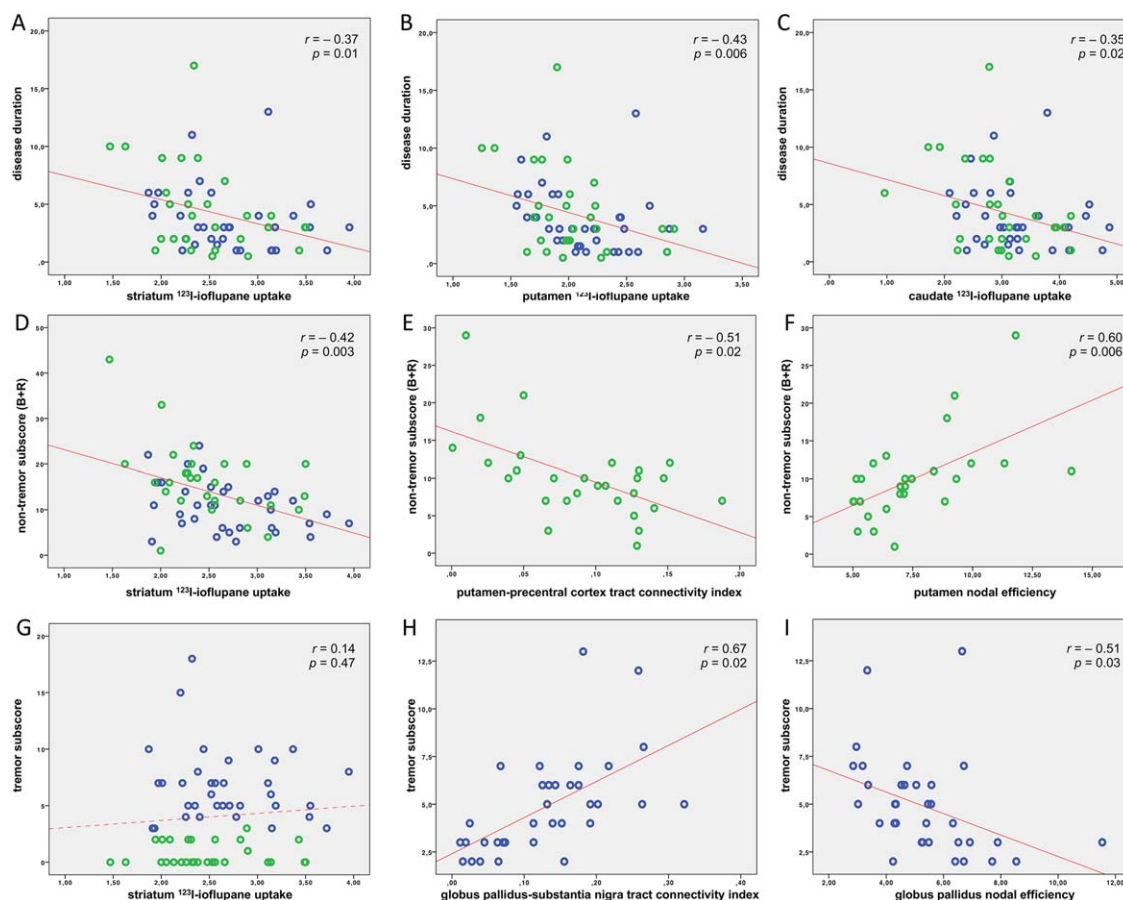


Figure 3.

Correlation analysis. Correlation scatterplots of the clinical variables [disease duration (A–C), nontremor subscore (D–F), and tremor subscore (G–I)] with the functional and structural neuroimaging metrics of more affected side, in all PD patients (A–C, D, G), in NT-PD patients (E, F), and in TD-PD patients (H, I). UPDRS-ME subscores in PD subgroups (panels E, F and panels H, I) are, respectively, the nontremor and tremor subscores of

more severely affected limbs. ^{123}I -ioflupane uptake ratios and MRI network metrics (i.e., anatomical connectivity indices and weighted nodal efficiency values) are reported on the *x* axis; clinical data are reported on the *y* axis; blue = patients with TD-PD; green = patients with NT-PD; *r* = Spearman's correlation coefficient; *P* = *P* value corrected according to false discovery rate. [Color figure can be viewed at wileyonlinelibrary.com]

control subjects, which reflects presynaptic deficit on DAT-SPECT and provides indirect evidence of the segmentation method reliability. Indeed, TD-PD and NT-PD patients displayed significantly higher values of substantia nigra weighted nodal efficiency in both sides. This increase of nigral nodal efficiency in patients with PD, regardless of the clinical phenotype, could be interpreted as a reflection of the nigral connectivity loss that constitutes the major pathologic degeneration of PD. According to the inclusion criteria of our study, all PD patients had an abnormal functional neuroimaging of the presynaptic dopaminergic system on DAT-SPECT, and striatal ^{123}I -ioflupane uptakes were correlated with the disease duration and the severity of bradykinesia and rigidity, but not with tremor. These results confirm that ^{123}I -ioflupane uptake is a good marker

to monitor severity and progression of PD [Benamer et al., 2000], and that the tremor severity does not depend on the striatal dopamine depletion [Kaasinen et al., 2014; Rossi et al., 2010]. The dopaminergic neuron loss in the substantia nigra pars compacta with the consequent dopamine depletion in the striatum (nigro-striatal dysfunction) [Kish et al., 1988; Pirker, 2003] is responsible for bradykinesia and rigidity, through a deafferentation of cortical motor area such as the supplementary motor area [Buhmann et al., 2003; Haslinger et al., 2001; Rascol et al., 1992; Wu et al., 2010], motor, and premotor cortices [Rowe et al., 2010; Sabatini et al., 2000].

This model, however, does not fully explain PD-associated tremor [Helmich et al., 2012; Kaasinen et al., 2014; Rossi et al., 2010], that is relatively independent of

TABLE III. Correlations of clinical variables with functional and structural neuroimaging parameters (i.e., ¹²³I-ioflupane uptakes and MRI graph metrics, respectively) in all 63 patients with Parkinson's disease

	Disease duration		UPDRS-ME		Tremor subscore		Nontremor subscore (B+R)		Axial subscore	
	rho	<i>P</i> value	rho	<i>P</i> value	rho	<i>P</i> value	rho	<i>P</i> value	rho	<i>P</i> value
¹²³I-ioflupane uptakes										
Specific/nonspecific ratios										
LAS putamen	-0.42	0.006	-0.45	0.006	0.13	0.47	-0.52	0.003	-0.32	0.03
MAS putamen	-0.43	0.006	-0.40	0.006	0.08	0.65	-0.48	0.006	-0.24	0.15
LAS caudate nucleus	-0.36	0.02	-0.31	0.03	0.23	0.17	-0.44	0.006	-0.22	0.18
MAS caudate nucleus	-0.35	0.02	-0.30	0.06	0.19	0.18	-0.41	0.006	-0.23	0.16
LAS striatum	-0.39	0.01	-0.48	0.006	0.10	0.57	-0.54	0.003	-0.35	0.02
MAS striatum	-0.37	0.01	-0.33	0.03	0.14	0.47	-0.42	0.003	-0.25	0.13
MRI network metrics										
Anatomical connectivity indices										
MAS globus pallidus–substantia nigra tract	0.08	0.72	0.13	0.47	0.37	0.02	0.02	0.95	0.21	0.18
MAS globus pallidus–thalamus tract	-0.29	0.06	-0.31	0.06	0.05	0.78	-0.33	0.03	-0.10	0.57
MAS putamen–precentral cortex tract	-0.40	0.006	-0.11	0.57	0.29	0.06	-0.19	0.18	-0.09	0.64
MAS thalamus–precentral cortex tract	-0.01	1.0	-0.22	0.18	0.17	0.34	-0.21	0.18	0.16	0.34
MAS caudate nucleus–supplementary motor area tract	0.03	0.87	-0.07	0.72	0.35	0.02	-0.27	0.08	-0.08	0.72
Weighted nodal efficiency values										
MAS globus pallidus	-0.19	0.18	-0.21	0.18	-0.43	0.006	-0.05	0.77	-0.11	0.57
MAS putamen	0.17	0.34	0.20	0.18	-0.10	0.57	0.14	0.47	0.24	0.16
MAS supplementary motor area	-0.06	0.78	-0.10	0.64	-0.22	0.18	-0.01	1.0	-0.06	0.72
MAS substantia nigra	-0.09	0.65	0.09	0.64	0.10	0.64	-0.01	0.95	0.06	0.78
LAS substantia nigra	-0.05	0.77	0.03	0.86	0.07	0.72	0.01	1.0	-0.01	1.0

rho = Spearman's correlation coefficient. Significant *P* values corrected for multiple comparisons (false discovery rate correction) are indicated in bold.

other cardinal signs [Zetuský et al., 1985], is less reliably responsive to dopaminergic modulation [Marjama-Lyons and Koller, 2000], and does not worsen at the same rate as bradykinesia and rigidity [Louis et al., 1999; Jankovic and Kapadia, 2001; Zetuský et al., 1985]. Emerging evidence suggests that other basal ganglia, such as the globus pallidus, could be involved in generating resting tremor. In this regard, we found that in TD-PD patients, the tremor severity correlated with the pallidal connectivity metrics indicating the relative integrity of pallidal connections. Indeed, in these patients, tremor subscores of more severely affected limbs were related with higher connectivity indices of nigro-pallidal tract, and with lower values of weighted nodal efficiency of the globus pallidus. Taken together, our findings suggest that the relative integrity of pallidal connectivity may contribute to the tremorgenesis in patients with TD-PD by an imbalance in favor of the dopaminergic excitatory influence [Rajput et al., 2008]. Although caution should be taken in attempting to relate these findings without further inquiry, this hypothesis seems to be in accordance with the evidence that pallidal deep brain stimulation [De Bie et al., 1999; Lozano et al., 1995; Vitek et al., 2004] or pallidotomy [Lozano et al., 1998] can lead to a consistent relief from resting tremor in PD patients with this prevalent motor sign.

There are some limitations to this study. First, the use of ROI-based probabilistic tractography may be criticized because of the a priori selection of nodes. However, when this technique is used with whole brain approach, the risk of reconstructing spurious connections may be high, thus making the results uncertain [Bonilha et al., 2015; Neher et al., 2015]. Moreover, on the basis of widely accepted evidences of a cortico-basal-ganglia and cerebello-thalamo-cortical involvement in PD patients reported in fMRI studies [Helmich et al., 2011; Lewis et al., 2011; Prodoehl et al., 2013], we included the main areas of this motor network. Second, the substantia nigra was identified by using a MRI-derived probabilistic atlas [Murty et al., 2014]. However, the resulting ROIs on each subject were visually assessed on T2-weighted images by one trained radiologist to exclude misregistration or erroneous identification. Third, the patients that assumed dopaminergic therapy were assessed clinically in the “practically off” condition. This may have minimized their scores of disability and reduced the sensitivity of clinical correlations, because of the long-duration response to levodopa [Zappia et al., 1997, 1999]. Finally, the probabilistic tractography algorithm did not include correction for path length, which may lead to distal false negatives in longer reconstructed tracts [Liptrot et al., 2014]. However, in agreement with

TABLE IV. Correlations between UPDRS-ME subscores of more severely affected limbs and the functional and structural neuroimaging parameters (i.e., ¹²³I-ioflupane uptakes and MRI network metrics, respectively) in Parkinson's disease subgroups

	Tremor subscore		Nontremor subscore (B + R)	
	rho	P value	rho	P value
¹²³I-ioflupane uptakes				
Specific/nonspecific ratios				
TD-PD (n = 35)				
LAS putamen	-0.34	0.27	-0.54	0.006
MAS putamen	-0.15	0.75	-0.50	0.02
LAS caudate nucleus	-0.25	0.29	-0.31	0.17
MAS caudate nucleus	-0.13	0.76	-0.26	0.18
LAS striatum	-0.28	0.29	-0.44	0.03
MAS striatum	-0.14	0.75	-0.39	0.05
NT-PD (n = 28)				
LAS putamen	0.07	0.83	-0.56	0.01
MAS putamen	0.01	1.0	-0.58	0.006
LAS caudate nucleus	0.08	0.83	-0.42	0.08
MAS caudate nucleus	0.06	0.91	-0.58	0.006
LAS striatum	0.09	0.83	-0.68	0.006
MAS striatum	0.03	0.99	-0.52	0.02
MRI network metrics				
Anatomical connectivity indices				
TD-PD patients (n = 35)				
MAS globus pallidus–substantia nigra tract	0.67	0.02	0.15	0.56
AS globus pallidus–thalamus tract	-0.29	0.29	-0.22	0.30
MAS putamen–precentral cortex tract	-0.14	0.75	0.24	0.30
MAS thalamus–precentral cortex tract	-0.34	0.27	-0.26	0.18
MAS caudate nucleus–supplementary motor aretract	-0.34	0.21	-0.06	0.80
NT-PD patients (n = 28)				
MAS globus pallidus–substantia nigra tract	-0.14	0.76	-0.06	0.88
MAS globus pallidus–thalamus tract	-0.07	0.83	-0.34	0.18
MAS putamen–precentral cortex tract	0.07	0.83	-0.51	0.02
MAS thalamus–precentral cortex tract	0.10	0.83	0.13	0.64
MAS caudate nucleus–supplementary motor area tract	NA	NA	NA	NA
Weighted nodal efficiency				
TD-PD (n = 35)				
MAS globus pallidus	-0.51	0.03	-0.26	0.18
MAS putamen	-0.01	1.0	-0.28	0.18
MAS supplementary motor area	-0.34	0.27	-0.17	0.44
MAS substantia nigra	0.14	0.76	0.22	0.30
LAS substantia nigra	-0.29	0.29	-0.07	0.80
NT-PD (n = 28)				
MAS globus pallidus	-0.14	0.76	-0.01	1.0
MAS putamen	0.23	0.74	0.60	0.006
MAS supplementary motor area	0.19	0.74	0.09	0.80
MAS substantia nigra	0.33	0.29	0.15	0.64
LAS substantia nigra	-0.18	0.75	0.01	1.0

rho = Spearman's correlation coefficient; NA = not applicable. The correlation of anatomical connectivity indices of the caudate nucleus–supplementary motor area tract and UPDRS-ME subscores was not applicable because this tract could not be reconstructed in any patient with nontremor Parkinson's disease. Significant P values corrected for multiple comparisons (false discovery rate correction) are indicated in bold.

recent studies [Zhong et al., 2015; Zhan et al., 2015] demonstrating the reliability of this method even without length correction, we were able to detect significant group

differences also in long subcortico-cortical connections. Further studies will be warranted to assess the influence of this aspect on this kind of analysis.

CONCLUSIONS

Our study demonstrates that probabilistic tractography is a technique able to highlight differences in the structure of the motor network between tremulous and nontremulous PD phenotypes. In particular, structural connectivity alterations of cortico-basal ganglia pathways occurred in NT-PD patients but not in TD-PD patients, suggesting that these anatomical differences may explain at least in part the clinical heterogeneity of PD.

ACKNOWLEDGMENTS

The authors report no conflict of interest.

The authors are grateful to patients and controls that kindly participated in the study.

REFERENCES

- Aarsland D, Andersen K, Larsen JP, Lolk A, Kragh-Sorensen P (2003): Prevalence and characteristics of dementia in Parkinson disease – An 8-year prospective study. *Arch Neurol* 60: 387–392.
- Achard S, Bullmore E (2007): Efficiency and cost of economical brain functional networks. *PLoS Comput Biol* 3:e17.
- Behrens TE, Berg HJ, Jbabdi S, Rushworth MF, Woolrich MW (2007): Probabilistic diffusion tractography with multiple fibre orientations: What can we gain?. *Neuroimage* 34:144–155.
- Behrens TE, Woolrich MW, Jenkinson M, Johansen-Berg H, Nunes RG, Clare S, Matthews PM, Brady JM, Smith SM (2003): Characterization and propagation of uncertainty in diffusion-weighted MR imaging. *Magn Reson Med* 50:1077–1088.
- Benamer HT, Patterson J, Wyper DJ, Hadley DM, Macphee GJ, Grosset DG (2000): Correlation of Parkinson's disease severity and duration with ¹²³I-FP-CIT SPECT striatal uptake. *Mov Disord* 15:692–698.
- Benjamini Y, Hochberg Y (1995): Controlling the false discovery rate: A practical and powerful approach to multiple testing. *J R Stat Soc Ser B Methodol* pp 289–300.
- Berardelli A, Rothwell JC, Thompson PD, Hallett M (2001): Pathophysiology of bradykinesia in Parkinson's disease. *Brain* 124: 2131–2146.
- Bonilha L, Gleichgerrcht E, Fridriksson J, Rorden C, Breedlove JL, Nesland T, Paulus W, Helms G, Focke NK (2015): Reproducibility of the structural brain connectome derived from diffusion tensor imaging. *PLoS One* 10:e0135247.
- Bostan AC, Dum RP, Strick PL (2010): The basal ganglia communicate with the cerebellum. *Proc Natl Acad Sci USA* 107: 8452–8456.
- Buhmann C, Glauche V, Sturenburg HJ, Oechsner M, Weiller C, Buchel C (2003): Pharmacologically modulated fMRI—cortical responsiveness to levodopa in drug-naïve hemiparkinsonian patients. *Brain* 126:451–461.
- Buijink AW, van der Stouwe AM, Broersma M, Sharifi S, Groot PF, Speelman JD, Maurits NM, van Rootselaar AF (2015): Motor network disruption in essential tremor: A functional and effective connectivity study. *Brain* 138:2934–2947.
- Bullmore E, Sporns O (2009): Complex brain networks: Graph theoretical analysis of structural and functional systems. *Nat Rev Neurosci* 10:186–198.
- Burn DJ, Rowan EN, Allan LM, Molloy S, O'Brien JT, McKeith IG (2006): Motor subtype and cognitive decline in Parkinson's disease, Parkinson's disease with dementia, and dementia with Lewy bodies. *J Neurol Neurosurg Psychiatry* 77:585–589.
- Darcourt J, Booij J, Tatsch K, Varrone A, Vander Borgh T, Kapucu OL, Nägren K, Nobili F, Walker Z, Van Laere K (2010): EANM procedure guidelines for brain neurotransmission SPECT using (123)I-labelled dopamine transporter ligands, version 2. *Eur J Nucl Med Mol Imag* 37:443–450.
- De Bie RMA, Schuurman PR, de Haan PS, Bosch DA, Speelman JD (1999): Unilateral pallidotomy in advanced Parkinson's disease: A retrospective study of 26 patients. *Mov Disord* 14:951–957.
- DeLong MR, Wichmann T (2015): Basal ganglia circuits as targets for neuromodulation in Parkinson disease. *JAMA Neurol* 72: 1354–1360.
- Dirkx MF, den Ouden H, Aarts E, Timmer M, Bloem BR, Toni I, Helmich RC (2016): The cerebral network of Parkinson's tremor: An effective connectivity fMRI study. *J Neurosci* 36: 5362–5372.
- Fahn S, Elton R, Members of the UPDRS Development Committee (1987): Recent Developments in Parkinson's Disease. Vol 2. Florham Park, NJ: Macmillan Health Care Information.
- Folstein MF, Folstein SE, McHugh PR (1975): "Mini-mental state". A practical method for grading the cognitive state of patients for the clinician. *J Psychiatr Res* 12:189–198.
- Foltyniec T, Brayne C, Barker RA (2002): The heterogeneity of idiopathic Parkinson's disease. *J Neurol* 249:138–145.
- Goetz CG, Tanner CM, Stebbins GT, Buchman AS (1988): Risk-factors for progression in Parkinson's disease. *Neurology* 38:1841–1844.
- Haber SN (2016): Corticostriatal circuitry. *Dialogues Clin Neurosci* 18:7–21.
- Haslinger B, Erhard P, Kämpfe N, Boecker H, Rummey E, Schwaiger M, Conrad B, Ceballos-Baumann AO (2001): Event-related functional magnetic resonance imaging in Parkinson's disease before and after levodopa. *Brain* 124:558–570.
- Helmich RC, Hallett M, Deuschl G, Toni I, Bloem BR (2012): Cerebral causes and consequences of parkinsonian resting tremor: A tale of two circuits?. *Brain* 135:3206–3226.
- Helmich RC, Janssen MJ, Oyen WJ, Bloem BR, Toni I (2011): Pallidal dysfunction drives a cerebellothalamic circuit into Parkinson tremor. *Ann Neurol* 69:269–281.
- Hoehn MM, Yahr MD (1967): Parkinsonism: Onset, progression and mortality. *Neurology* 17:427–442.
- Hughes AJ, Daniel SE, Kilford L, Lees AJ (1992): Accuracy of clinical diagnosis of idiopathic Parkinson's disease: A clinico-pathological study of 100 cases. *J Neurol Neurosurg Psychiatry* 55:181–184.
- Jankovic J, Kapadia AS (2001): Functional decline in Parkinson disease. *Arch Neurol* 58:1611–1615.
- Jankovic J, McDermott M, Carter J, Gauthier S, Goetz C, Golbe L, Huber S, Koller W, Olanow C, Shoulson I, Stern M, Tanner C, Weiner W and Parkinson Study Group (1990): Variable expression of Parkinson's disease: A base-line analysis of the DATATOP cohort. The Parkinson Study Group. *Neurology* 40:1529–1534.
- Jellinger KA, Paulus W (1992): Clinico-pathological correlations in Parkinson's disease. *Clin. Neurol Neurosurg* 94:S86–S88.
- Jenkinson M, Beckmann CF, Behrens TE, Woolrich MW, Smith SM (2012): FSL. *NeuroImage* 62:782–790.
- Kaasinen V, Kinos M, Joutsa J, Seppänen M, Noponen T (2014): Differences in striatal dopamine transporter density between tremor dominant and non-tremor Parkinson's disease. *Eur J Nucl Med Mol Imag* 41:1931–1937.

- Kish SJ, Shannak K, Hornykiewicz O (1988): Uneven pattern of dopamine loss in the striatum of patients with idiopathic Parkinson's disease. Pathophysiologic and clinical implications. *N Engl J Med* 318:876–880.
- Langston JW, Widner H, Goetz CG, Brooks D, Fahn S, Freeman T, Watts R (1992): Core assessment program for intracerebral transplantations (CAPIT). *Mov Disord* 7:2–13.
- Lewis MM, Du G, Sen S, Kawaguchi A, Truong Y, Lee S, Mailman RB, Huang X (2011): Differential involvement of striato- and cerebello-thalamo-cortical pathways in tremor- and akinetic/rigid-predominant Parkinson's disease. *Neuroscience* 177:230–239.
- Lewis SJ, Foltynie T, Blackwell AD, Robbins TW, Owen AM, Barker RA (2005): Heterogeneity of Parkinson's disease in the early clinical stages using a data driven approach. *J Neurol Neurosurg Psychiatry* 76:343–348.
- Lindvall O, Björklund A (1979): Dopaminergic innervation of the globus pallidus by collaterals from the nigrostriatal pathway. *Brain Res* 172:169–173.
- Liptrot MG, Sidaros K, Dyrby TB (2014): Addressing the path-length-dependency confound in white matter tract segmentation. *PLoS One* 9:e96247.
- Louis ED, Tang MX, Cote L, Alfaro B, Mejia H, Marder K (1999): Progression of parkinsonian signs in Parkinson disease. *Arch Neurol* 56:334–337.
- Lozano AM, Lang AE, Galvez-Jimenez N, Miyasaki J, Duff J, Hutchinson WD, Dostrovsky JO (1995): Effect of GPi pallidotomy on motor function in Parkinson's disease. *Lancet* 346:1383–1387.
- Lozano AM, Lang AE, Hutchison WD (1998): Pallidotomy for tremor. *Mov Disord* 13:107–110.
- Marjama-Lyons J, Koller W (2000): Tremor-predominant Parkinson's disease. Approaches to treatment. *Drugs Aging* 16:273–278.
- Michely J, Volz LJ, Barbe MT, Hoffstaedter F, Viswanathan S, Timmermann L, Eickhoff SB, Fink GR, Grefkes C (2015): Dopaminergic modulation of motor network dynamics in Parkinson's disease. *Brain* 138:664–678.
- Murty VP, Shermohammed M, Smith DV, Carter RM, Huettel SA, Adcock RA (2014): Resting state networks distinguish human ventral tegmental area from substantia nigra. *NeuroImage* 100:580–589.
- Neher PF, Descoteaux M, Houde JC, Stieltjes B, Maier-Hein KH (2015): Strengths and weaknesses of state of the art fiber tractography pipelines—A comprehensive in-vivo and phantom evaluation study using tractometer. *Med Image Anal* 26:287–305.
- Nicoletti A, Pugliese P, Nicoletti G, Arabia G, Annesi G, Mari MD, Lamberti P, Grasso L, Marconi R, Epifanio A, Morgante L, Cozzolino A, Barone P, Torchia G, Quattrone A, Zappia M (2010): Voluptuary habits and clinical subtypes of Parkinson's disease: The FRAGAMP case-control study. *Mov Disord* 25:2387–2394.
- Obeso JA, Rodriguez-Oroz MC, Stamelou M, Bhatia KP, Burn DJ (2014): The expanding universe of disorders of the basal ganglia. *Lancet* 384:523–531.
- Parent A, Lavoie B, Smith Y, Bédard P (1990): The dopaminergic nigropallidal projection in primates: Distinct cellular origin and relative sparing in MPTP-treated monkeys. *Adv Neurol* 53:111–116.
- Parkinson J (1817): *An Essay on the Shaking Palsy*. London: Sherwood, Neely, and Jones, Paternoster Row.
- Patenaude B, Smith SM, Kennedy DN, Jenkinson M (2011): A Bayesian model of shape and appearance for subcortical brain segmentation. *NeuroImage* 56:907–922.
- Pelzer EA, Hintzen A, Goldau M, von Cramon DY, Timmermann L, Tittgemeyer M (2013): Cerebellar networks with basal ganglia: Feasibility for tracking cerebello-pallidal and subthalamo-cerebellar projections in the human brain. *Eur J Neurosci* 38:3106–3114.
- Pirker W (2003): Correlation of dopamine transporter imaging with parkinsonian motor handicap: How close is it? *Mov Disord* 18:S43–S51.
- Prodoehl J, Planetta PJ, Kurani AS, Comella CL, Corcos DM, Vaillancourt DE (2013): Differences in brain activation between tremor- and non-tremor-dominant Parkinson disease. *JAMA Neurol* 70:100–106.
- Rajput AH, Sitte HH, Rajput A, Fenton ME, Pifl C, Hornykiewicz O (2008): Globus pallidus dopamine and Parkinson motor subtypes: Clinical and brain biochemical correlation. *Neurology* 70:1403–1410.
- Rascol O, Sabatini U, Chollet F, Celsis P, Montastruc JL, Marc-Vergnes JP, Rascol A (1992): Supplementary and primary sensory motor area activity in Parkinson's disease. Regional cerebral blood flow changes during finger movements and effects of apomorphine. *Arch Neurol* 49:144–148.
- Rossi C, Frosini D, Volterrani D, De Feo P, Unti E, Nicoletti V, Kiferle L, Bonuccelli U, Ceravolo R (2010): Differences in nigro-striatal impairment in clinical variants of early Parkinson's disease: Evidence from a FP-CIT SPECT study. *Eur J Neurol* 17:626–630.
- Rowe JB, Hughes LE, Barker RA, Owen AM (2010): Dynamic causal modelling of effective connectivity from fMRI: Are results reproducible and sensitive to Parkinson's disease and its treatment? *NeuroImage* 52:1015–1026.
- Sabatini U, Boulanouar K, Fabre N, Martin F, Carel C, Colonnese C, Bozzao L, Berry I, Montastruc JL, Chollet F, Rascol O (2000): Cortical motor reorganization in akinetic patients with Parkinson's disease: A functional MRI study. *Brain* 123:394–403.
- Sharman M, Valabregue R, Perlberg V, Marrakchi-Kacem L, Vidailhet M, Benali H, Brice A, Lehericy S (2013): Parkinson's disease patients show reduced cortical-subcortical sensorimotor connectivity. *Mov Disord* 28:447–454.
- Tomlinson CL, Stowe R, Patel S, Rick C, Gray R, Clarke CE (2010): Systematic review of levodopa dose equivalency reporting in Parkinson's disease. *Mov Disord* 25:2649–2653.
- Vitek JL, Hashimoto T, Peoples J, DeLong MR, Bakay RAE (2004): Acute stimulation in the external segment of the globus pallidus improves parkinsonian motor signs. *Mov Disord* 19:907–915.
- Wen W, Zhu W, He Y, Kochan NA, Reppermund S, Slavin MJ, Brodaty H, Crawford J, Xia A, Sachdev P (2011): Discrete neuroanatomical networks are associated with specific cognitive abilities in old age. *J Neurosci* 31:1204–1212.
- Williams-Gray CH, Foltynie T, Brayne CE, Robbins TW, Barker RA (2007): Evolution of cognitive dysfunction in an incident Parkinson's disease cohort. *Brain* 130:1787–1798.
- Wu T, Wang L, Hallett M, Li K, Chan P (2010): Neural correlates of bimanual anti-phase and in-phase movements in Parkinson's disease. *Brain* 133:2394–2409.
- Zappia M, Bosco D, Plastino M, Nicoletti G, Branca D, Oliveri RL, Aguglia U, Gambardella A, Quattrone A (1999): Pharmacodynamics of the long-duration response to levodopa in PD. *Neurology* 53:557–560.
- Zappia M, Colao R, Montesanti R, Rizzo M, Aguglia U, Gambardella A, Oliveri RL, Quattrone A (1997): Long-duration

response to levodopa influences the pharmacodynamics of short-duration response in Parkinson's disease. *Ann Neurol* 42:245–248.

Zetuský WJ, Jankovic J, Pirozzolo FJ (1985): The heterogeneity of Parkinson's disease: Clinical and prognostic implications. *Neurology* 35:522–526.

Zhan L, Zhou J, Wang Y, Jin Y, Jahanshad N, Prasad G, Nir TM, Leonardo CD, Ye J, Thompson PM, For the Alzheimer's

Disease Neuroimaging Initiative (2015): Comparison of nine tractography algorithms for detecting abnormal structural brain networks in Alzheimer's disease. *Front Aging Neurosci* 14:7:48.

Zhong S, He Y, Gong G (2015): Convergence and divergence across construction methods for human brain white matter networks: An assessment based on individual differences. *Hum Brain Mapp* 36:1995–2013.